Paste 2026 – AB Fourie, M Horta, M Oliveira & S Wilson (eds)

doi:10.36487/ACG_repo/2655_04

Stability analysis of filtered tailings stack slopes in Brazil using building information modelling and advanced work packaging

Thiago Franklin Santos de Almeida [a,*], Alison Souza Norberto [a], Matheus Lima Barros [a], João Lucas Vieira Andrade [a], Guilherme Dias Santos Amaral Iff Jannuzzi [a]

[a] TPF Engenharia, Brazil

Abstract

The ongoing digital transformation in the mining industry has accelerated the integration of building information modelling (BIM) and advanced work packaging (AWP) into geotechnical engineering workflows, enabling more efficient planning, risk assessment, and data management. This paper presents a case study on the application of BIM and AWP to the design and stability assessment of a filtered tailings stack within a digitally managed construction sequencing plan. The workflow included georeferencing, quality control of field surveys, digitalisation of geological–geotechnical data, and the generation of 3D geotechnical modelling was performed using Autodesk Civil 3D (Autodesk 2024) and Seequent Leapfrog Geo (Seequent 2024), while stability analyses were carried out using Slide2 and RS2 developed by Rocscience (2024a, 2024b). Applying limit equilibrium method (LEM) and finite element method (FEM) approaches. The BIM–AWP integration enabled automated extraction of representative cross-sections at each construction stage and direct linkage between digital sequencing and geotechnical analyses, improving traceability, interdisciplinary coordination, and decision-making throughout the project lifecycle. The results indicate that both LEM and FEM analyses yielded safety factors and strength reduction factors consistently above regulatory thresholds, confirming high static and deformation stability of the structure. This performance is primarily attributed to the gentle slope geometry (1V:3H) and the relatively high strength parameters of the filtered tailings. The findings demonstrate that digitally integrated geotechnical workflows enhance the reliability of staged stability evaluations and provide practical insights into the evolution of deformation mechanisms during construction, supporting safer, more efficient, and environmentally responsible tailings management practices.

Keywords: *filtered tailings stack, BIM, AWP, stability analysis, digital geotechnical workflow*

1 Introduction

Digital transformation in the mining industry has intensified over the past few decades, driven by the growing need for more sustainable and efficient practices. Among the key technological innovations that have emerged, building information modelling (BIM) and advanced work packaging (AWP) stand out as crucial tools that enhance integrated planning, geotechnical risk assessment, and resilience in project delivery.

Previous studies indicate that the application of BIM facilitates more effective project management by providing a digital model that enhances visualisation, simulation, and analysis of construction data (Eastman et al. 2011). In turn, AWP organises work into sequenced packages, promoting a systematic approach that improves execution and coordination among the teams and disciplines involved (Construction Industry Institute 2020).

[*] Corresponding author. Email address: thiago.almeida@tpfe.com.br

Waste management – particularly concerning filtered tailings storage facilities – poses a significant challenge for the industry, especially in countries like Brazil where regulatory and environmental standards have strengthened. The safe and sustainable storage of waste is essential to mitigate geotechnical and environmental risks associated with landslides and structural failures, which can result in devastating impacts on the environment and local communities (Global Tailings Review, International Council on Mining and Metals, United Nations Environment Programme & Principles for Responsible Investment 2021). In this context, the use of advanced modelling and analysis techniques, such as those offered by BIM and AWP, emerges as a necessity to ensure the structural integrity of the facilities.

The limit equilibrium method (LEM) and the finite element method (FEM) are essential for stability analyses of mining structures, as they enable a detailed assessment of the safety conditions. LEM is related to the principles of statics, assuming in most cases a circular slip surface and calculating the forces in slices. In contrast, FEM allows for more precise analysis, accounting for displacements and stress (Burman et al. 2015), which enables simulations that reflect the behaviour of a tailing stack under different loading conditions.

This study presents a practical case illustrating the integrated application of BIM and AWP for the design and stability verification of a filtered tailings stack in Brazil. From the construction sequencing, analyses were conducted using LEM and FEM to determine the safety factor (SF) and identify critical scenarios. The main contribution of this study lies in the direct integration of BIM-based construction sequencing with staged geotechnical stability analyses using both LEM and FEM. Unlike conventional approaches, the proposed workflow automatically links 3D digital models to representative 2D sections extracted at each construction stage, enabling continuous evaluation of SFs and deformation mechanisms throughout the stacking process. This integration provides practical insights into how stability evolves during operational sequencing, supporting decision-making, construction planning, and geotechnical risk management in filtered tailings facilities.

2 Methodology

The methodology adopted in this study was structured to integrate the stages of construction sequencing, digital modelling, and geotechnical stability analyses applied to a filtered tailings stack. The activities were organised into sequential stages that encompass defining geometry and the execution plan, integrating the construction phases into the digital model, and conducting comparative analyses between the limit equilibrium and stress–strain methods. This approach aims to ensure a comprehensive and integrated view of the filtered tailings stack, providing technical support for project optimisation, risk management, and the establishment of geotechnical monitoring guidelines throughout the structure's lifecycle.

2.1 Integration of the sequencing of the analysis steps

The definition of the general geometry of the filtered tailings stack was the starting point for the integration between construction sequencing and stability analyses. The geometric configuration was established based on the topographic boundaries of the area and the geotechnical foundation conditions, considering the compatibility between the operational slopes, intermediate berms, and the surface drainage system. Figure 1 below presents an overview of the filtered tailings stack.

From the consolidated geometry, a plan of disposal was defined which presents the projection of the volume of material to be placed over time in the study area, integrating the aspects of BIM and AWP to organise the lifecycle of the structure into successive construction stages or construction work areas. Autodesk Civil 3D (Autodesk 2024) was used mainly for the modelling works of geotechnical structures and Seequent Leapfrog for the geological strata (Seequent 2024). Input data included georeferenced data of satellite images, contours and geological–geotechnical data.

This planning covers the stages of stacking, drainage, access implementation, and closure, allowing for progressive control of field activities. In the case analysed, the filtered tailings stack is situated in a valley region, and due to this geomorphological configuration, the disposal of tailings was conducted using the ascending method. The digital model enabled the sequencing of activities in time and space, ensuring

coherence between physical execution and geotechnical performance analyses. The BIM model provided a consistent basis for the evolutionary assessment of stability during the different construction stages in 3D, as shown in Figure 2, with the accumulated volume and height along the years of operation. It is important to note that the linear relationship between time and disposed volume shown in the graph represents a simplified illustration of the construction sequencing. In practice, placement rates may vary according to operational constraints, material availability, and geotechnical conditions. The linear representation is intended solely to support visualisation of the staging concept adopted in this study.

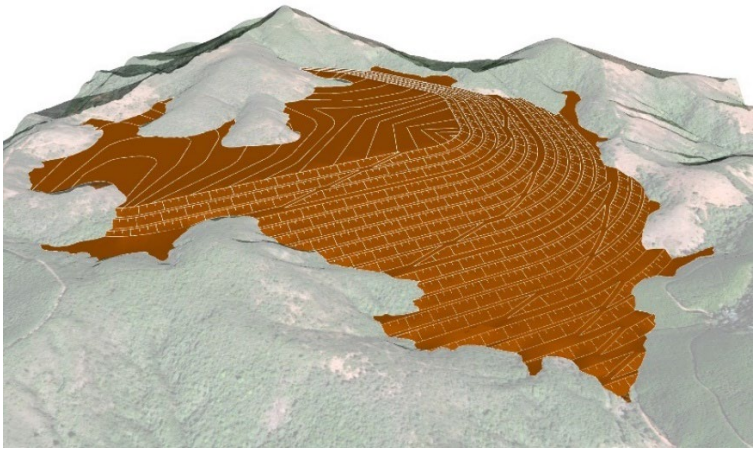

Figure 1 General geometry of the filtered tailings stack

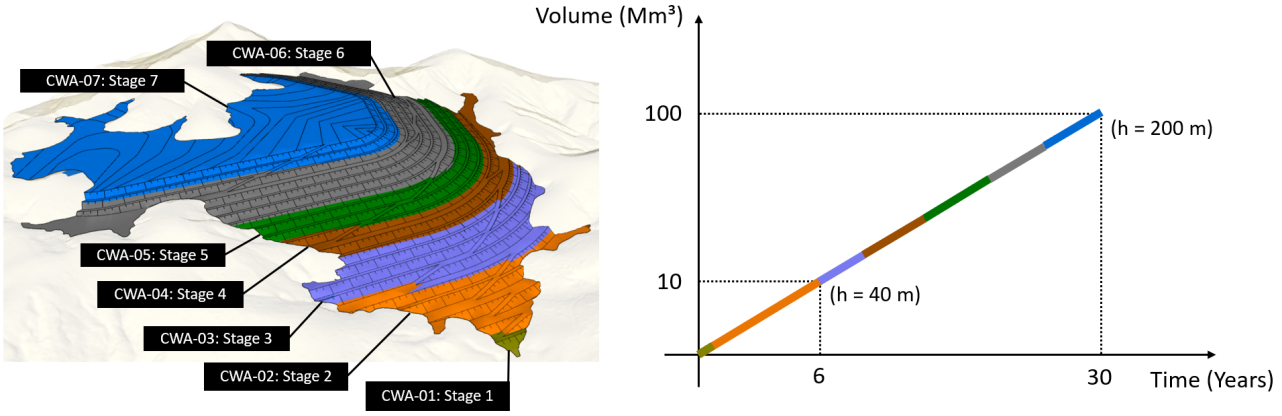

Figure 2 Sequencing graph (building information modelling and advanced work packaging and plan of disposal; h = height)

The link between the BIM model and the execution plan was fundamental in defining the analysis milestones and the representative section. Each construction stage was associated with a set of typical sections, generated automatically from the BIM model and exported to geotechnical analysis software. The section was selected to represent the most significant geometric variations of the filtered tailings stack, including stretches of natural foundation, transition zones, and areas of maximum stacking (Figure 3).

This integration between digital sequencing and geotechnical analysis stages ensured traceability between construction phases and stability results, making it possible to evaluate the evolution of the SF as stacking progress and according to the projected operational conditions.

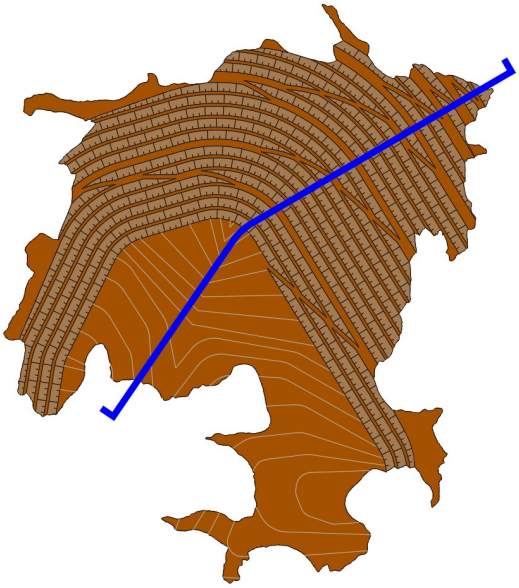

Figure 3 Location of the section analysed in the building information modelling model

2.2 Stability analyses

The stability analyses were conducted progressively, following the stages defined in the construction sequencing of the filtered tailings stack. The aim was to assess the variation of global stability conditions throughout the stacking process and to identify the critical zones associated with each construction stage, presented in Figure 4.

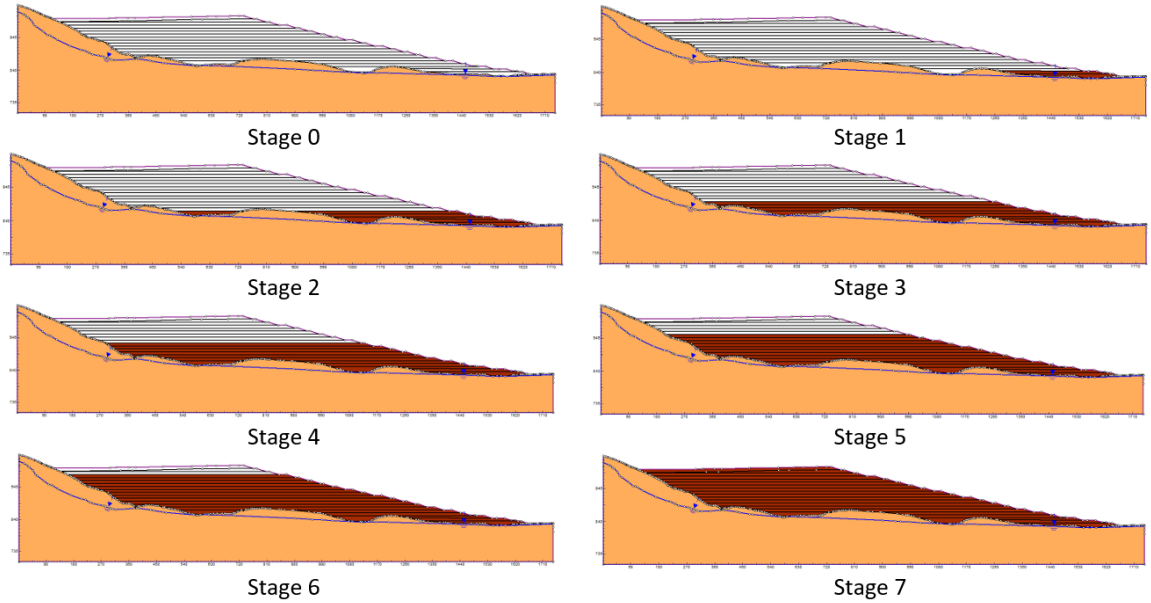

Figure 4 Representation of the analysis steps throughout the sequencing (red = filtered tailings, orange = foundation)

For the stability verification, representative parameters of shear strength and deformability of the materials comprising the filtered tailings stack and its foundation were adopted. The tailings were considered as a mixture composed of 100% sandy tailings and 100% ultrafine mass (sludge), corresponding to an equivalent ratio of 80% sandy fraction and 20% fine fraction, reflecting the typical condition of the filtered material after the mixing and disposal process. The strength and deformability parameters for the materials are presented in Table 1.

Table 1 Resistance and deformability parameters adopted in the analyses

Material	Colour	γ (kN/m³)	c' (kPa)	ϕ' (°)	E (MPa)	ν (–)	Constitutive model
Filtered tailings		21	0	32	22	0.3	Mohr–Coulomb
Foundation		19	10	35	45	0.3	

The strength parameters adopted for the filtered tailings (c′ = 0; ϕ′ = 32°; γ = 21 kN/m³) were selected to represent well-compacted, partially drained filtered tailings, consistent with the construction methodology and internal drainage conditions of the stack. Published studies indicate that compacted filtered tailings typically exhibit friction angles ranging between 30 and 35° (Bhanbhro 2014; Islam et al. 2023), while effective cohesion is commonly assumed negligible for drained or dry tailings materials (Baecher 1983). In this study, a friction angle of 32° was deliberately adopted near the lower bound of reported values, providing a conservative yet representative estimate of shear strength for conceptual-level analyses.

Deformability parameters were defined based on experimental evidence for compacted fine tailings and granular foundation materials. An elastic modulus of E = 22 MPa and a Poisson's ratio of ν = 0.3 were adopted, consistent with published ranges indicating stiffness values between 10 and 50 MPa depending on moisture content, density, and stress history (Campana & Verdugo 2013; Demoz et al. 2022). The selected modulus represents an intermediate value within this range, reflecting moderate compaction and partial drainage conditions expected during construction. Seismic and laboratory investigations further demonstrate that stiffness increases with higher dry density and reduced void ratio (Liew & Xiao 2019; Santos et al. 2025), supporting the adoption of relatively elevated stiffness values for filtered tailings stacks constructed under controlled placement conditions.

Although site-specific laboratory testing was not available at this conceptual stage, the adopted parameters are consistent with internationally reported ranges and were selected to provide a realistic and technically defensible representation of material behaviour for comparative LEM–FEM stability assessment.

Extreme rainfall scenarios and associated transient pore pressure conditions were not explicitly modelled in this study, as the primary focus was on construction sequencing and staged stability under typical operational conditions for filtered tailings. However, the proposed BIM-integrated LEM–FEM framework allows straightforward incorporation of such scenarios, including elevated water contents and sensitivity analyses on material parameters, which are recommended for subsequent design phases.

The methodological approach for determining the critical failure surface combined the LEM, through the determination of the SF, and the FEM, based on the strength reduction factor (SRF). The LEM analyses were performed using the Slide2 software, while the FEM simulations were conducted in RS2, both developed by Rocscience (2024a, 2024b). This integrated approach enabled a direct comparison between the 2 methods and facilitated the identification of potential critical instability zones, correlating them with the successive construction stages of filtered tailings stack. Furthermore, the results of the numerical analyses provide a foundation for establishing geotechnical monitoring guidelines, focusing on the regions most susceptible to variations in stress and displacement throughout the operational lifespan of the structure.

In the analyses conducted by the LEM, a minimum depth filter of 10 m was applied to search for potential rupture surfaces. This restriction aimed to eliminate the generation of shallow or local surfaces, which typically represent small-scale surface instabilities and are not representative of the global behaviour of the structure. The adoption of this criterion allowed for a focus on deeper and more critical rupture surfaces associated with the global stability of the filtered tailings stack, ensuring greater consistency and reliability in the interpretation of the SFs obtained.

In the analyses conducted by the FEM, mechanical boundary conditions were applied, and a mesh composed of triangular finite elements with secondary nodes was adopted, as illustrated in Figure 5. It is noteworthy that the analyses by the FEM considered the sequencing of the disposal in layers of 10 m.

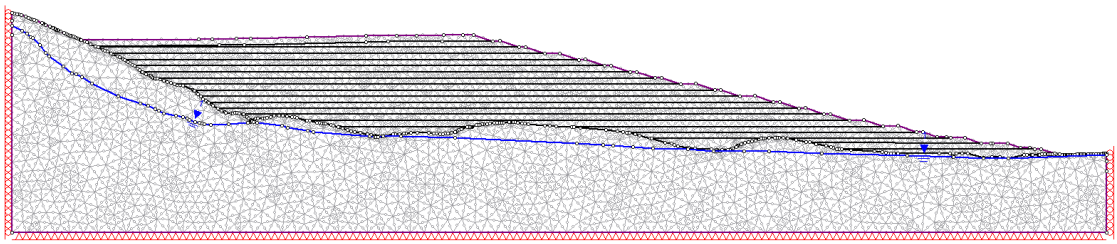

Figure 5 Mesh model and boundary conditions used in stress-strain analyses

A fixed low groundwater table was assumed across all construction stages, consistent with the drained conditions expected in filtered tailings operations and the presence of internal drainage systems. This simplification was adopted to focus on the influence of geometry and staged loading on stability. The proposed framework allows incorporation of transient hydraulic conditions in future analyses, including rainfall scenarios and variable saturation.

The combination of results obtained from the LEM and FEM methods will allow for a more comprehensive assessment of the behaviour of the filtered tailings stack, from both a static safety perspective and a deformation response perspective, providing technical support for the calibration of stability criteria and the enhancement of the monitoring system in operation.

Although based on an applied engineering project, this study emphasises analytical interpretation of staged stability behaviour rather than procedural documentation. Descriptions were streamlined to highlight methodological integration and key geotechnical insights derived from the combined LEM–FEM assessment.

3 Results and discussion

In terms of results, although both factors (SF and SRF) remained at elevated levels across all stages, the initial numerical difference was notable, as seen in Stage 1 (SF = 2.44 and SRF = 3.40) (Figure 6), highlighting the complementary role of the FEM in providing insight into the deformation response, while the LEM focuses on static safety. In terms of geometric comparison, the wedges calculated by both methods displayed similar behaviour in this stage, concentrating on the berms and within the filtered tailings layer.

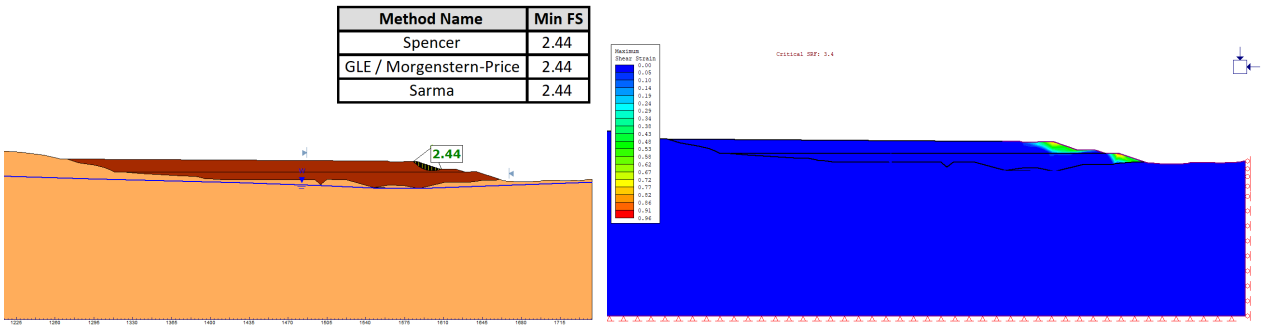

(a) (b)

Figure 6 Stage 1: comparison of the critical rupture surfaces of the limit equilibrium method analyses from the determination of the safety factor (SRF) and finite element method from the determination of the strength reduction factor (SRF). (a) SF = 2.44; (b) SRF = 3.40

For Stage 2, with the addition of 3 more layers of 10 m each, the SF from the LEM increased to 2.81, while the SRF from the FEM reduced to 2.60 (Figure 7). In terms of correlation, this convergence between the factors suggests that the mass began to develop more cohesive and predictable stress behaviour. Geometrically, the critical failure surface from the LEM shifted to the slope face, and the shear band from the FEM also showed a clear concentration in this same region.

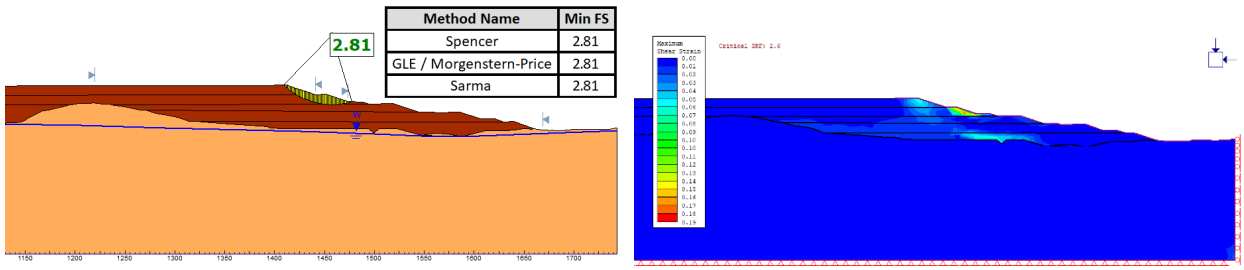

(a) (b)

Figure 7 Stage 2: comparison of the critical rupture surfaces of the limit equilibrium method analyses from the determination of the safety factor (SF) and finite element method from the determination of the strength reduction factor (SRF). (a) SF = 2.81; (b) SRF = 2.60

In Stage 3 (Figure 8), corresponding to the addition of 3 new layers of filtered tailings stack, it was observed that the increase in vertical stresses resulting from the elevating structure tended to maintain the SF at high levels, albeit with a possible slight decrease or stabilisation. In this condition, SF = 3.19 and SRF = 2.60 were obtained. From the geometric perspective, the analyses from the FEM indicated a deepening of the potential failure surfaces within the tailings body, extending into the contact zone with the foundation. This behaviour reflects the increase in the total mass of the embankment and characterises a transition in the failure mechanism from this stage when the filtered tailings stack reaches an approximate global height of 80 m. On the other hand, the analysis from the LEM presented a failure surface predominantly superficial, confined to the intermediate region of the filtered tailings stack, between several berms, suggesting less mobilisation of deep volumes compared to the FEM.

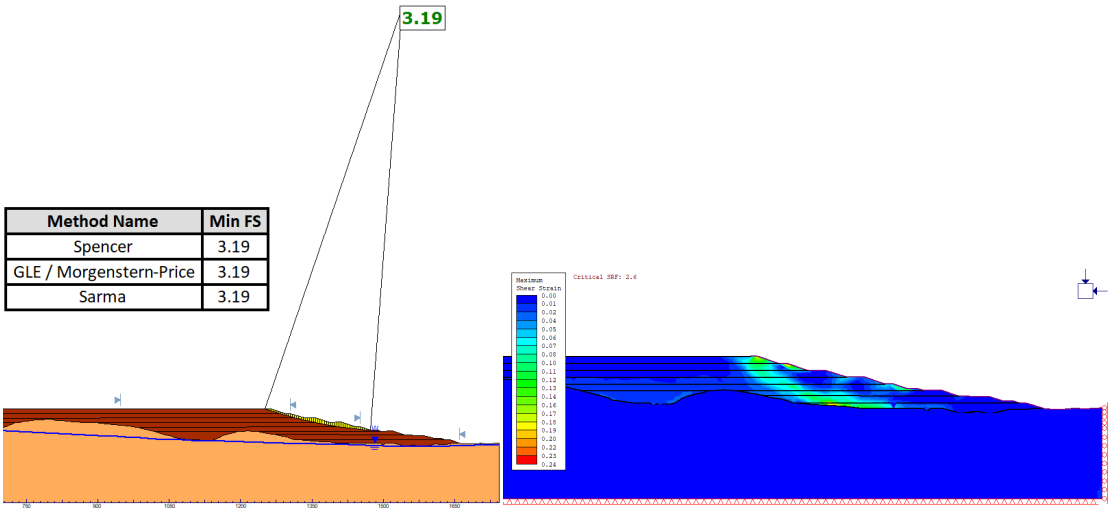

(a) (b)

Figure 8 Stage 3: comparison of the critical rupture surfaces of the limit equilibrium method analyses from the determination of the safety factor (SF) and finite element method from the determination of the strength reduction (SRF). (a) SF = 3.19; (b) SRF = 2.60

In Stage 4, the values obtained were SF = 2.88 (LEM) and SRF = 2.60 (FEM) (Figure 9). From the geometric perspective, the analysis from the FEM indicated that the failure surface remained deep; however, the deformation field revealed concentrations of displacements in the upper portion of the slope, an aspect that requires attention in field monitoring. In turn, the analysis from the LEM maintained a predominantly superficial failure surface, with a slight deepening of the wedge compared to the previous stages.

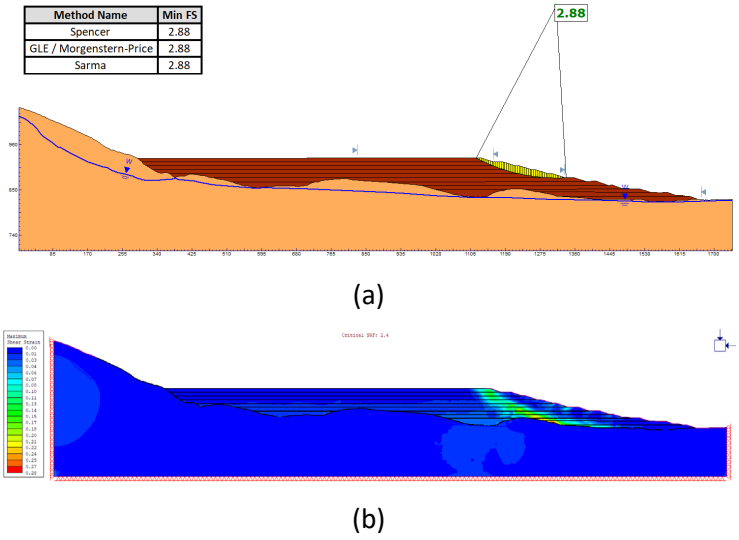

(a)

(b)

Figure 9 Stage 4: comparison of the critical rupture surfaces of the limit equilibrium method analyses from the determination of the safety factor (SF) and finite element method from the determination of the strength reduction factor (SRF). (a) SF = 2.88; (b) SRF = 2.40

In Stage 5, SF = 2.97 (LEM) and SRF = 2.40 (FEM) were obtained (Figure 10). From the geometric perspective, the analysis from the FEM indicated that the failure surface remained deep, presenting similar numerical magnitude and geometric configuration to those of Stage 4. This repetition of behaviour suggests a convergence trend of the critical wedge, associated with the gradual accumulation of deformations throughout the construction sequencing of the filtered tailings stack, an aspect that deserves special attention in field monitoring. On the other hand, the analysis from the LEM showed that the failure surface remained predominantly superficial, indicating localised stability in the upper portions of the slope.

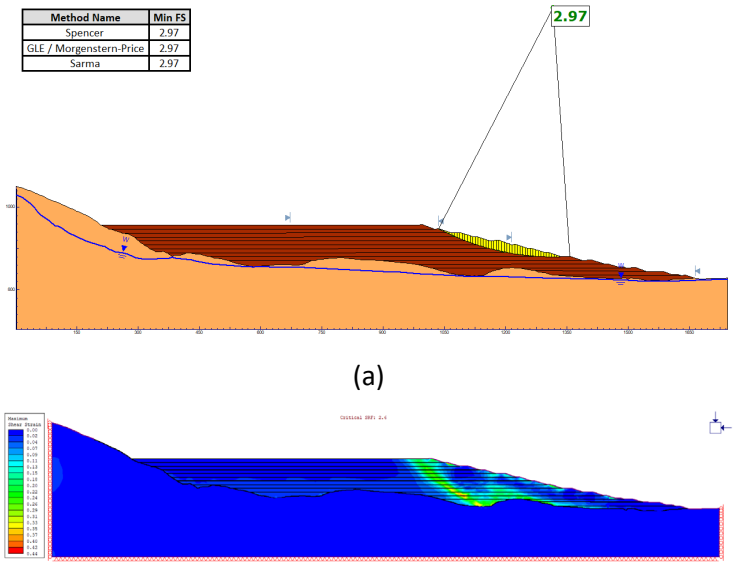

(a)

(b)

Figure 10 Stage 5: comparison of the critical rupture surfaces of the limit equilibrium method analyses from the determination of the safety factor (SF) and finite element method from the determination of the strength reduction factor (SRF). (a) SF = 2.97; (b) SRF = 2.40

In Stage 6, SF = 2.82 (LEM) and SRF = 2.40 (FEM) were obtained (Figure 11). The analysis from the FEM evidenced the maintenance of a deep failure surface, consistent with the behaviour observed in previous stages, indicating stabilisation of the global deformation mechanism throughout the construction evolution.

This pattern suggests that the critical wedge reached a practically consolidated configuration, without significant variations in geometry or SRF. Meanwhile, the analysis from the LEM continued to indicate superficial failures restricted to the berms, reinforcing the local criticality of these analyses.

In Stage 7, SF = 2.83 (LEM) and SRF = 2.40 (FEM) were obtained (Figure 12). The analysis from the FEM confirmed the persistence of a deep failure surface, maintaining the pattern observed in previous stages. This constancy in results indicates that the filtered tailings stack has entered a stable behaviour regime, with the SRF showing a tendency toward stabilisation. Conversely, the analysis from the LEM continued to identify shallow and localised failures between the berms, which reinforces the local and secondary nature of these potential instabilities compared to the global response of the structure.

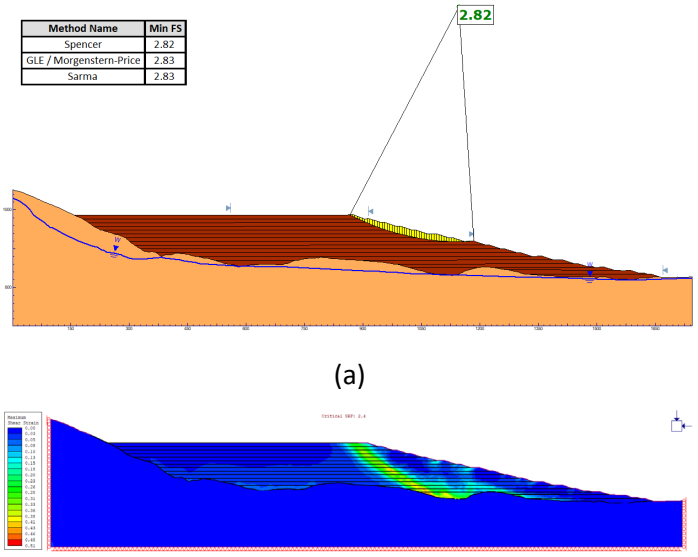

(a)

(b)

Figure 11 Stage 6: comparison of the critical rupture surfaces of the limit equilibrium method analyses from the determination of the safety factor (SF) and finite element method from the determination of the strength reduction factor (SRF). (a) SF = 2.82; (b) SRF = 2.40

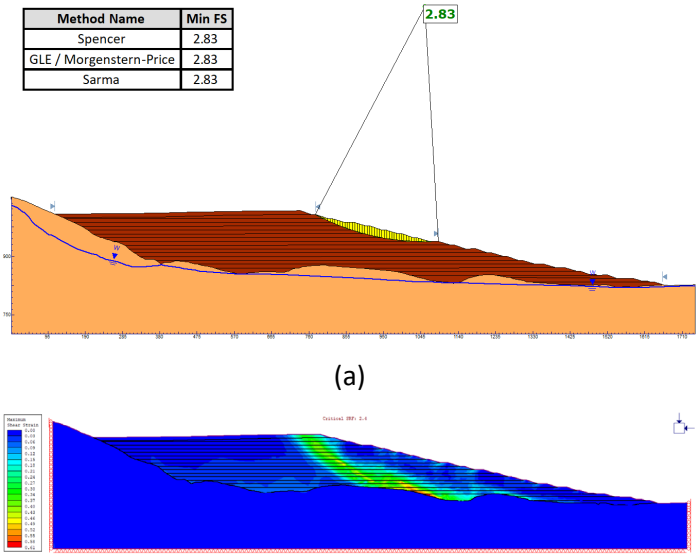

(a)

(b)

Figure 12 Stage 7: comparison of the critical rupture surfaces of the limit equilibrium method analyses from the determination of the safety factor (SF) and finite element method from the determination of the strength reduction factor (SRF). (a) SF = 2.83; (b) SRF = 2.40

Overall, the integrated analysis process, combining the results from the LEM and FEM, demonstrated that the filtered tailings stack under study exhibits high levels of static and deformation stability throughout all construction stages. This condition is strongly associated with the favourable geometry of the filtered tailings stack, especially the gentle slope inclinations, as well as the relatively high strength parameters adopted for the tailings. In numerical terms, the SF obtained from the LEM and the SRF derived from the FEM consistently remained above the minimum values normally recommended for structures of this type, confirming the robustness of both the geometric arrangement and the internal drainage conditions. Table 2 presents a summary of the results obtained for each construction stage, including the values of SF, SRF, and the location of the critical rupture surfaces identified by each method.

Table 2 Summary of the results of the analysis of rupture surfaces by limit equilibrium method (LEM) and finite element method (FEM). SF = safety factor; SRF = safety reduction factor

Stage	LEM		FEM	
	SF	Critical rupture surface	SRF	Critical rupture surface
1	2.44	Shallow slip surface between berms (local failure)	3.40	Shallow slip surface between berms (local failure)
2	2.81	Shallow slip surface between berms (local failure)	2.60	Shallow slip surface between berms (local failure)
3	3.19	Shallow slip surface between berms (global failure)	2.60	Stack–foundation interface (global failure)
4	2.88	Shallow slip surface between berms (global failure)	2.40	Stack–foundation interface (global failure)
5	2.97	Shallow slip surface between berms (global failure)	2.40	Stack–foundation interface (global failure)
6	2.82	Shallow slip surface between berms (global failure)	2.40	Stack–foundation interface (global failure)
7	2.83	Shallow slip surface between berms (global failure)	2.40	Stack–foundation interface (global failure)

In summary, the results from Table 2 reveal a trend of stabilisation of the SRF values around 2.40 from Stage 4 onwards; a behaviour that indicates the establishment of a stable regime of stress and deformation redistribution within the mass. This stability is consistent with the geometric evolution of the filtered tailings stack as after the initial growth stages, the global failure mechanism consolidates with more pronounced mobilisation at the interface between the body of the filtered tailings stack and the foundation. On the other hand, the analyses from the LEM indicated failure surfaces predominantly located between berms, with a slight increase in SF up to Stage 3, followed by stabilisation. This difference between the methods reflects the expected behaviour: while the LEM tends to represent more superficial and localised instability mechanisms, the FEM can capture deformations distributed at greater depths, allowing for the identification of the progressive transition from local to global instability mechanisms throughout construction. These results reinforce the efficiency of the integrated approach and provide important insights for planning geotechnical monitoring and optimising the geometry of the filtered tailings stack.

The combination of the 2 analytical methodologies enhances the joint assessment of global equilibrium behaviour, represented by the LEM, and the deformation and stress mobilisation response, represented by the FEM. This integrated approach is widely recommended in the literature for stability studies of complex geotechnical structures, including dams and filtered tailings stack, as it provides a more comprehensive interpretation of mechanical performance over time (Ildefonso & Suarez 2024).

The differences observed between SF from LEM and SRF from FEM reflect the inherent distinctions between the 2 methods. LEM is mainly controlled by instantaneous geometry and predefined slip surfaces, whereas FEM accounts for stress redistribution and cumulative deformation during construction. As a result, intermediate stages show some divergence between SF and SRF, while FEM captures progressive stress mobilisation within the stack and at the stack–foundation interface.

In the final stages, the stabilisation of SRF values indicates consolidation of the critical deformation mechanism as the overall geometry approaches its ultimate configuration. This convergence suggests that the critical wedge reaches a quasi-steady state governed primarily by slope geometry and material properties. The combined use of LEM and FEM therefore provides complementary insight into both geometric stability and deformation-controlled behaviour.

4 Conclusion

The static and deformation stability study, conducted through the integration of LEM and FEM across 7 construction stages of a filtered tailings stack, highlighted key aspects of the global structural behaviour. Numerical results demonstrated that the stack maintains wide safety margins throughout all evaluated phases, with both SF and SRF consistently exceeding minimum values recommended by geotechnical guidelines. This elevated stability is attributed not only to the strength and stiffness of the filtered tailings, but also to the gentle overall slope geometry (1V:3H), which promotes stress dissipation and significantly reduces shear demand along the slopes.

Geometric analysis of potential failure surfaces provided relevant insight into dominant instability mechanisms, reinforcing the importance of comparative assessment between methods. FEM, by incorporating stress redistribution and cumulative deformation, identified deeper critical mechanisms extending toward the stack–foundation interface, whereas LEM indicated predominantly superficial surfaces between berms. These differences are technically significant, as they support prioritisation of instrumentation and monitoring zones, contributing to proactive geotechnical risk management.

The combined application of LEM and FEM proved essential for comprehensive stability evaluation, allowing static safety to be interpreted alongside deformation response throughout construction. In this study, the integration of BIM and AWP primarily provided qualitative benefits, including improved data traceability, interdisciplinary coordination, and automated extraction of representative sections for each construction stage. Although quantitative performance metrics were not formally assessed, the digital workflow strengthened alignment between construction sequencing and geotechnical analyses, supporting more informed design decisions.

Once construction and operations are underway, the proposed framework can be continuously updated using as-built geometries, field observations, and instrumentation data, enabling recalibration of numerical models and ongoing verification of stability conditions. This capability supports adaptive construction management and proactive control of geotechnical risks over the facility lifecycle. While the numerical results are site-specific, the integrated methodology is transferable to other filtered tailings projects, offering a scalable digital approach for safe, efficient, and sustainable tailings management.

References

Autodesk 2024, *Autodesk Civil 32: Comprehensive Detailed Design and Documentation Software for Civil Infrastructure*, viewed 8 February 2026, https://www.autodesk.com/products/civil-3d/overview

Baecher, GB, Consla, JA, Lin, JS & Marr, WA 1983, *Critical Parameters for Tailings Embankments*, Bureau of Mines Open File Report 135-83, Springfield, pp. 1–282, https://stacks.cdc.gov/view/cdc/206673

Bhanbhro, R 2014, *Mechanical Properties of Tailings and Tailings Paste for Backfill Design*, PhD thesis, Luleå University of Technology, Luleå, https://www.diva-portal.org/smash/get/diva2:989943/FULLTEXT01.pdf

Burman, A, Maity, D & Sahay, RR 2015, 'Comparative study of slope stability using limit equilibrium method and finite element method', *International Journal of Engineering Research and Technology*, vol. 4, no. 5, pp. 829–834.

Campana, JBE & Verdugo, R 2013, 'Shear strength and deformation modulus of tailing sands under high pressures', *Proceedings of the 18th International Conference on Soil Mechanics and Geotechnical Engineering.*

Construction Industry Institute 2020, *AWP Education Framework (Version 1.0)*, AWP Education & Outreach Subcommittee.

Demoz, A 2022, 'Geotechnical properties determination of thickened fluid fine tailings', *Geotechnical and Geological Engineering*, vol. 40, pp. 1887–1898, https://doi.org/10.1007/s10706-021-01998-3

Eastman, C, Teicholz, P, Sacks, R, & Liston, K 2011, 'BIM Handbook: A Guide to Building Information Modeling for Owners, Managers, Designers, Engineers, and Contractors', John Wiley & Sons, Hoboken.

Global Tailings Review, International Council on Mining and Metals, United Nations Environment Programme & Principles for Responsible Investment 2021, *Global Industry Standard on Tailings Management*, viewed 8 February 2026, https://globaltailingsreview.org/wp-content/uploads/2020/08/global-industry-standard_EN.pdf

Ildefonso, N & Suarez, J 2024, 'Evaluation of the stress history in a tailings dam raising stages: A study based on finite element method (FEM) methodology', *Proceedings of the 9th International Conference on Civil Structural and Transportation Engineering,* https://doi.org/10.11159/iccste24.206

Islam, MR, Santos, R & Alves, M 2023, 'A study on the mechanical behaviour of three different fine mine tailings', *Journal of King Saud University - Engineering Sciences*, vol. 35, issue 5, pp. 335–341, https://doi.org/10.1016/j.jksues.2021.04.001

Liew, M & Xiao, M 2019, 'In situ seismic investigations of coal tailings', *Geotechnical Special Publication,* American Society of Civil Engineers, vol. 2019-March, n. GSP 311, pp. 239-247, viewed 8 Feb 2026, https://doi.org/10.1061/9780784482131.025

Rocscience 2024a, *RS2*, computer software, viewed 8 February 2026, https://www.rocscience.com/software/rs2

Rocscience 2024b, *Slide 2*, computer software, viewed 8 February 2026, https://www.rocscience.com/software/slide2

Santos, RA, Vulpe, C, Fourie, A, Jefferies, M, Silva, JPS & Casagrande, MDT 2025, 'Shear wave velocity and small-strain stiffness across a broad range of states in iron ore tailings', *Canadian Geotechnical Journal*, vol. 62, pp. 1–18, viewed 8 February 2026, https://doi.org/10.1139/cgj-2024-0751

Sequeent 2024, *Leapfrog Geo*, computer software, viewed 8 February 2026, https://www.seequent.com/products-solutions/leapfrog-geo/